Observations of the absorption, infra-red emission, and excitation spectra of Cr in $BaTiO_3$

1998 J. Phys.: Condens. Matter 10 10775

(http://iopscience.iop.org/0953-8984/10/47/021)

J. Phys.: Condens. Matter **10** (1998) 10775–10786. Printed in the UK PII: S0953-8984(98)92527-9

Observations of the absorption, infra-red emission, and excitation spectra of Cr in $BaTiO_3$

S Eden†, S Kapphan†, H Hesse†, V Trepakov‡, V Vikhnin‡, I Gregora§, L Jastrabik§ and J Seglins‖

† FB Physik, University of Osnabrück, 49069 Osnabrück, Germany
‡ A F Ioffe Physical-Technical Institute, RAS, 194 021 St Petersburg, Russia
§ Institute of Physics, Academy of Science of the Czech Republic, 180 40 Prague 8, Czech Republic
‖ University of Riga, Kengaraga 8, Riga, Latvia

Received 17 March 1998, in final form 24 August 1998

Abstract. Photoluminescence and optical absorption in Cr-doped $BaTiO_3$ were observed for the first time and studied within the 300–800 nm spectral region and over a 7–300 K temperature range. 'Nominally pure' $BaTiO_3$ crystals, with Cr impurities detected by means of EPR, and intentionally Cr-doped $BaTiO_3$ crystals grown by the top-seeded solution method were studied. Cr doping results in additional absorption over the whole visible region, increasing towards the band-edge area (at ≈400 nm), and wide absorption bands centred at about 470 nm, 575 nm, and 610 nm. At 74 K, exposure to optical excitation with $\lambda_{exc} = 400$ nm results in luminescence in the near-infra-red region consisting of four sharp lines, A_1 (781.65 nm, 12 795 cm^{-1}), A_2 (776.4 nm, 12 879 cm^{-1}), A_3 (768.8 nm, 13 005 cm^{-1}), A_4 (766.8 nm, 13 039 cm^{-1}), and several additional weak emission lines. The luminescence excitation spectrum for each A line consists of two complex bands centred at 630 nm (15 873 cm^{-1}) and at 400 nm (25 000 cm^{-1}) for $T = 74$ K. With decreasing temperature, all of the sharp lines, such as the $R_{1,2}$ zero-phonon lines of Cr^{3+} in $SrTiO_3$, shift to lower energies, which is opposite to the behaviour of such lines for ionic crystals. The thermal shift for the A_2 line is the largest, ≈0.12 cm^{-1} K^{-1}. Taking into consideration EPR data, temperature transformations, and the lifetime of the sharp emission lines (≈1 ms at 70 K), we argue that the A_3 and A_4 lines are $R_{1,2}$ lines, i.e. originating from zero-phonon $^2E \rightarrow {}^4A_2$ transitions of single Cr^{3+} ions replacing Ti^{4+} ions. The nature of the $A_{1,2}$ emission lines is not quite clear, but can be considered to originate from Cr^{3+} ions exchange coupled with other, unknown defects (including Cr^{3+} exchange-coupled pairs) or with $^2E \rightarrow {}^4A_2$-type transitions of Cr^{3+} centres perturbed by nearest-site hole polarons, O^- or OH^-.

1. Introduction

Understanding the structure and the properties of intrinsic and extrinsic defects in barium titanate, $BaTiO_3$, is of great interest because of the technological importance of this ferroelectric material. The attractive optical properties of Cr impurity centres have been widely studied for Cr in other perovskite-like ABO_3 and related materials: $SrTiO_3$ [1–3], $KTaO_3$ [2–4], $LiNbO_3$ [5–9], $CaTiO_3$ [10], TiO_2 [11] and see the literature cited in these references. But so far Cr in $BaTiO_3$ has been studied mainly by the EPR technique [12–21]. It is surprising, in view of the attractive photorefractive properties of Cr-doped $BaTiO_3$ reported in [13, 22], revealing a Glass constant of $k_1 = 1.2 \times 10^{-8}$ A cm W^{-1}, which is an order of magnitude larger than that for $LiNbO_3$, that optical spectra of Cr impurity centres in $BaTiO_3$ have not been studied in detail yet. Only in reference [22] has the room

0953-8984/98/4710775+12$19.50

temperature absorption spectrum for 'heavily doped' $BaTiO_3$:Cr (20 ppm) been reported. As was shown, the doping with Cr is accompanied by two major effects in the absorption:

(i) the band edge is effectively moved toward lower energy, which gives the crystal its reddish colour; and

(ii) the absorption becomes more anisotropic.

Except for a broad shoulder at about 600 nm in the *c*-axis absorption, which has not been assigned to Cr^{3+} or other compensating defect transitions, there was no other structure seen in the absorption curves reported [22].

Additional interest in the study of the optical spectra of Cr in $BaTiO_3$ is connected with the possibility of an off-centre position of the Cr^{3+} ions incorporated at the Ti^{4+} lattice sites; such a possibility has been discussed in reference [12] for $BaTiO_3$ and in reference [3] for $SrTiO_3$. Indeed, in such cases, Cr^{3+} ($3d^3$, t_{2g}^3, $S = 3/2$) could be expected to participate strongly in the collective motion of the B-lattice ions responsible for the ferroelectricity. Cr^{3+} has only a t_{2g}^3 half-filled subshell, which is essentially antibonding, having its charge density pointing between the oxygen ions [12]. This could give rise to a Cr^{3+} position that is slightly off-centre, shifted along the ⟨100⟩ cubic directions, like that of Cr^{3+} in MgO [23]. Also, the effective repulsion of the first oxygen-ion sphere from the Cr^{3+} ion with decreasing overlap could be another off-centre driving mechanism [3]. Although the EPR data [12] demonstrate that Cr^{3+}, substituting for Ti^{4+} in $BaTiO_3$, remains centred in the octahedral cell (at least on average) in all ferroelectric phases, a weak off-centre behaviour can appear when a coherent tunnelling state is realized. Another possibility for off-centre behaviour of Cr^{3+} in $BaTiO_3$ can arise upon photoexcitation in the orbitally degenerate ^2E state, due to a Jahn–Teller effect—similar to that considered in reference [2, 3] for Cr^{3+} in $KTaO_3$ and $SrTiO_3$—causing an unusual zero-phonon-luminescence R-line behaviour as a function of temperature and electric field.

Here we report the first observation of and a discussion of optical absorption, photoluminescence, and excitation spectra of Cr in $BaTiO_3$.

2. Experimental procedure

The nominally pure crystals used in this investigation were four specimens of $BaTiO_3$: spontaneously crystallized butterfly-type crystals, designated as PC-246, Czochralski-grown PC-38, a top-seeded solution-grown (TSSG) [24] crystal K32, and a second TSSG specimen 57.2 that had been investigated earlier in reference [16]. In the latter specimen (57.2), the presence of Cr^{3+}, Cr^{4+}, and Cr^{5+} centres (identified in the ppm range) was established by means of EPR [16]. The doped $BaTiO_3$ single crystals with 100 ppm and 1000 ppm of Cr in the melt were top-seeded solution grown at the crystal growth laboratory of the University of Osnabrück. The specimens were oriented and cut along the ⟨100⟩ principal directions. The x-ray and optical microscopic analysis showed a good homogeneity of the Cr-doped samples. Here the main focus of attention was the red-tinted $BaTiO_3$ crystal with 100 ppm of Cr (R35) rather than the green-tinted crystal with 1000 ppm of Cr in the melt (GR81). On the basis of a preliminary chromium content analysis, following reference [12], it could be assumed that about a quarter of the chromium present in the melt is incorporated. The optical absorption measurements in the 300–800 nm region were performed using a Beckman ACTA VII double-beam spectrometer with the samples mounted in a refrigerator-cooled cryostat, ROK10-300 from Leybold. Emission and excitation photoluminescence spectra were recorded using a SPEX 1500 single-grating spectrometer with a cooled RCA C31034 GaAs photomultiplier and a photon-counting system (ORTEC). As the excitation source, an

XBO 300 W high-pressure Xe lamp and a SPEX Minimate as the variable-bandpass filter, with additional interference filters to minimize stray light effects, were used. The crystals were also mounted in a refrigerator-cooled cryostat, ROK10-300 from Leybold. For the luminescence lifetime measurements, the XBO light source was chopped and the photons were counted with the multi-channel scaler Model 914P from EG&G. Highly resolved luminescence spectra were measured using a SPEX-14018 double spectrometer with the spectral width of the slits set to about 0.1 cm^{-1}. As the excitation source a krypton laser (647.09 nm) was used, and the luminescence was detected with a standard photon-counting detector. Here, the specimens were mounted in a continuous-flow He cryostat (Leybold) with a He-exchange gas chamber. A conventional 9.2 GHz spectrometer was used to inspect the EPR spectra at 77 K. All of the optical experiments were performed in unpolarized light using polydomain samples.

3. Results and discussion

According to available EPR results [12–21], Cr in $BaTiO_3$ occurs as Cr^{3+}, Cr^{4+}, and Cr^{5+}. Cr^{3+} and Cr^{4+} occupy Ti^{4+} sites. Cr^{5+} is found in two modifications: on-site Cr^{5+}(I) replacing Ti^{4+}, and off-centre Cr^{5+}(II) which is surrounded by four O^{2-} ions as nearest neighbours; this is similar to the case of Cr^{5+}(I) and Cr^{5+}(II) in $SrTiO_3$ [25, 26]. Our control EPR spectra with $BaTiO_3$:Cr (100 ppm) in the rhombohedral phase at 77 K were in agreement with literature data, revealing a rather high concentration of Fe^{3+}, Cr^{5+}, and Cr^{3+} impurity centres at Ti^{4+} sites.

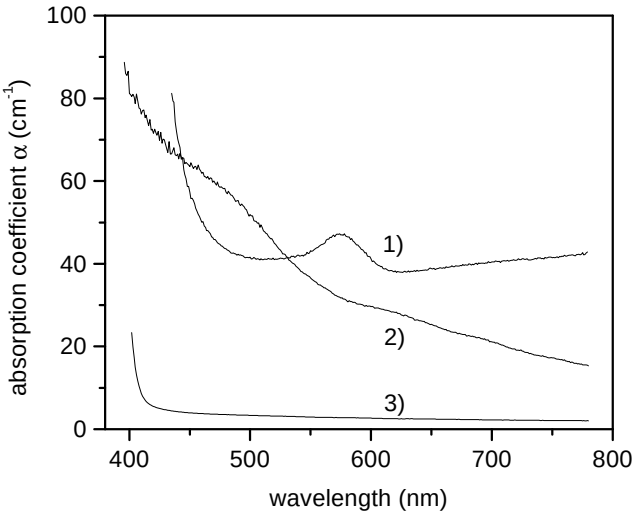

Figure 1. Absorption spectra of (1) $BaTiO_3$:Cr (1000 ppm, Gr81) at 13 K, (2) $BaTiO_3$:Cr (100 ppm, R35) at 13 K, and (3) a nominally pure $BaTiO_3$ crystal (57.2). The measurements were done using unpolarized light at room temperature.

3.1. Optical absorption

The nominal pure slightly yellow $BaTiO_3$ single crystals investigated are transparent in the visible region, with band-gap edge absorption $E_g \approx 3.06$ eV (405 nm) at room temperature. Tetragonal domains had no perceptible influence on the optical transmission. Figure 1 shows

unpolarized absorption spectra for nominally pure and Cr-doped $BaTiO_3$ crystals. Compared to that of nominally pure $BaTiO_3$, the total absorption of $BaTiO_3$:Cr in the visible region increases. Such an increasing of the absorption in the 400–600 nm region leads to the red colour of the 100 ppm Cr-doped sample (R35). The shift of the band edge to lower energies with increasing Cr content can be assumed to be connected with Cr^{6+} transitions, which can give rise to a strong UV absorption (at 380 nm in green $3CaO{\cdot}SiO_2$ [27]). In addition to those in the band-edge region, absorptions occur in the R35 crystal centred approximately at 470 nm and 610 nm. The more heavily doped $BaTiO_3$:Cr (1000 ppm, GR81) crystal shows an additional absorption band at 575 nm which is giving rise to the deep green colour of the specimen.

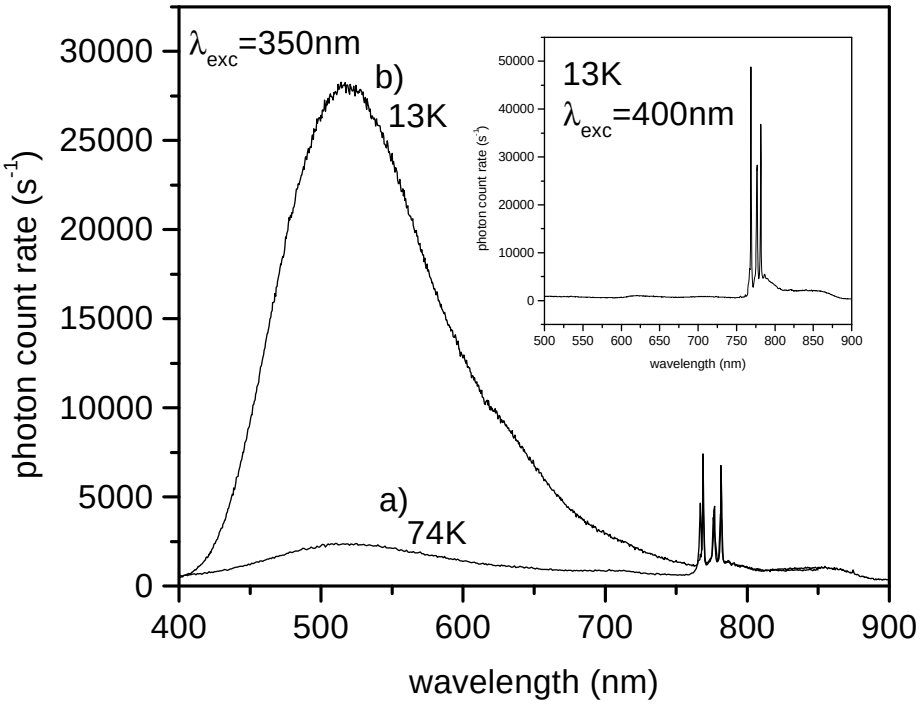

Figure 2. Luminescence emission spectra of a nominally pure $BaTiO_3$ (57.2) crystal under excitation at $\lambda = 350$ nm for (a) $T = 74$ K and (b) $T = 13$ K. The inset shows the spectrum excited at $\lambda = 400$ nm for $T = 13$ K.

3.2. Photoluminescence

Interband excitation of nominally pure $BaTiO_3$ (PC-246 and PC-38) crystals at $\lambda = 355$ nm results in the well-known visible wide-band emission with a maximum at 500 nm (at 23 K), as reported, e.g., in reference [28]. However, the nominally pure 57.2 specimen and Cr-doped $BaTiO_3$ (R35, GR81) together with the wide-band visible emission reveal a complex-structured luminescence in the near-IR region. Figures 2(a) and 2(b) show the luminescence spectrum of the $BaTiO_3$ nominally pure 57.2 specimen at 74 K and 13 K under excitation by light with $\lambda_{exc} = 350$ nm, and in the inset with $\lambda_{exc} = 400$ nm, at 13 K. It can be seen that interband excitation results in the structured IR and visible luminescence, which dominates at low temperatures. Light with $\lambda = 400$ nm excites the structured IR luminescence only

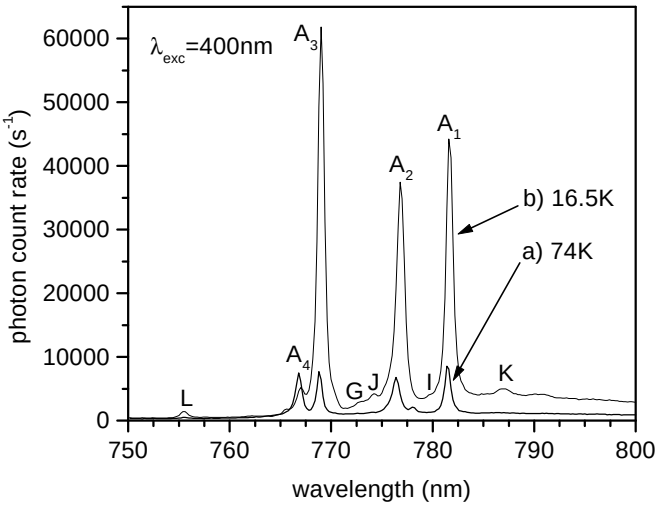

Figure 3. Infra-red luminescence emission spectra of $BaTiO_3$:Cr (100 ppm, R32) under excitation at $\lambda = 400$ nm for (a) $T = 74$ K and (b) $T = 16.5$ K.

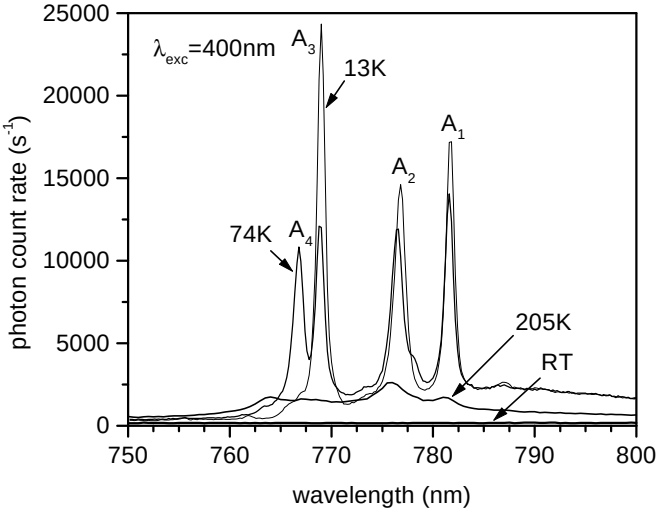

Figure 4. Infra-red luminescence emission spectra of $BaTiO_3$:Cr (1000 ppm, GR81) under excitation at $\lambda = 400$ nm for RT, $T = 205$ K, $T = 74$ K, and $T = 13$ K.

(see the inset in figure 2). It should be mentioned that for Cr-doped $BaTiO_3$ crystals the visible luminescence is weaker and the structured IR luminescence is much more pronounced than for nominally pure $BaTiO_3$. Figure 3 (curve (a)) presents details of the IR emission spectrum of $BaTiO_3$:Cr (100 ppm) at 74 K ($\lambda_{exc} = 400$ nm). It consists of four sharp lines (at 74 K): A_1 at 781.65 nm (12 795 cm^{-1} with halfwidth $\Delta\delta_{1/2} = 9$ cm^{-1}); A_2 centred at 776.4 nm (12 879 cm^{-1}, $\Delta\delta_{1/2} = 14$ cm^{-1}); and, looking like an obvious doublet, A_3 centred at 768.8 nm (13 005 cm^{-1}) and A_4 centred at 766.8 nm (13 039 cm^{-1}, these lines having equal halfwidths: $\Delta\delta_{1/2} = 13$ cm^{-1}). Besides the above, some weak emissions, I at 778.1 nm (12 852 cm^{-1}), J at 774.1 nm (12 918 cm^{-1}), G at 772.5 nm (12 945 cm^{-1}), and L at 755.5 nm (13 236 cm^{-1}), appear. Curve (b) of figure 3 shows the IR luminescence

spectrum for $BaTiO_3$:Cr (100 ppm) at $T = 16.5$ K. It shows that the total emission yield is increasing at low temperatures. Practically all of the luminescence lines which are observed at 74 K are also observed at 16.5 K, except the A_4 line which decreases in intensity drastically. The IR emission spectra of $BaTiO_3$:Cr (1000 ppm) at 13 K, 74 K, 205 K, and RT are shown in figure 4. A broadened weak-structured IR luminescence, within the region around 760–790 nm, is seen even at 205 K, intensifying strongly at lower temperatures. No change in the luminescence pattern was observed at the temperature of about 190 K where the phase transition between the orthorhombic and the rhombohedral phase takes place.

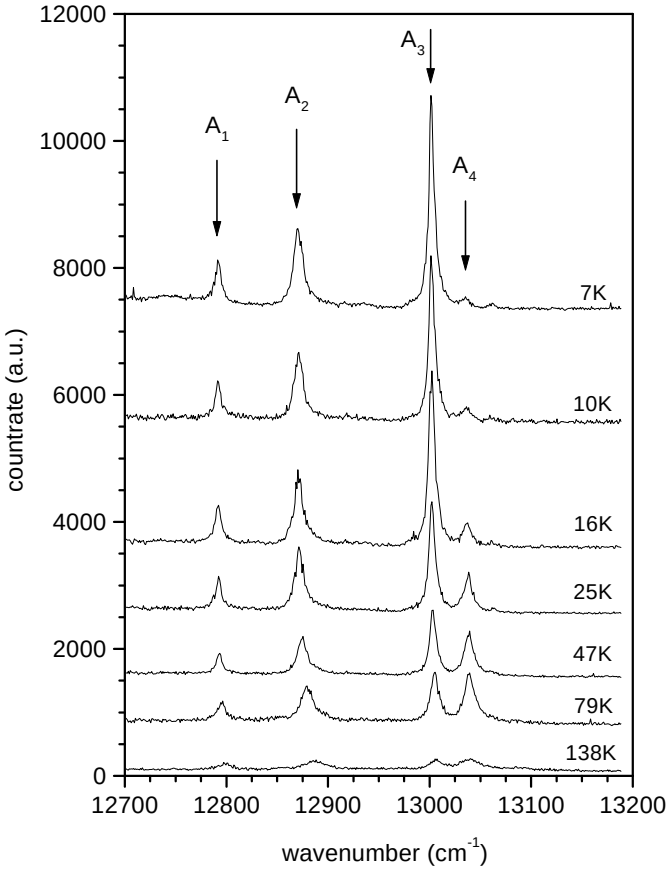

Figure 5. Highly resolved (better than 0.1 cm^{-1}) IR emission spectra of $BaTiO_3$:Cr (100 ppm, R32) at different temperatures excited by a krypton laser beam (647.09 nm).

Figure 5 shows the highly resolved (better than 0.1 cm^{-1}) IR emission spectra of $BaTiO_3$:Cr (100 ppm) at different temperatures, excited by a 647.09 nm krypton laser beam.

Table 1 summarizes the energies, halfwidths, and thermal shifts (between 7 K and 79 K) of the main emission lines observed in $BaTiO_3$:Cr (100 ppm).

The positions of all A lines shift to lower energies with decreasing temperature. The shift from 7 K to 79 K is nearly the same for the A_3 and A_4 lines, about 4 cm^{-1}, which means on average ≈ 0.055 cm^{-1} K^{-1}. The A_2 line shifts by about 8.5 cm^{-1} (≈ 0.12 cm^{-1} K^{-1}) and the A_1 line by about 3.5 cm^{-1} (≈ 0.049 cm^{-1} K^{-1}). Such a shift to low energy is

Table 1. Positions and halfwidths of the main IR emission lines at different temperatures in $BaTiO_3$:Cr (100 ppm) under Kr laser beam excitation (647.09 nm, $P = 200$ mW).

	A_1		A_2		A_3		A_4	
Temperature (K)	$h\nu$ (cm^{-1})	$\delta_{1/2}$	$h\nu$ (cm^{-1})	$\delta_{1/2}$	$h\nu$ (cm^{-1})	$\delta_{1/2}$	$h\nu$ (cm^{-1})	$\delta_{1/2}$
7	12 792	9	12 871	9	13 001	6	13 035	
10	12 792	8	12 871	11	13 001.5	8	13 036	
16	12 792	9	12 871	11	13 002	8	13 037	11
25	12 792.5	7	12 872	10	13 002.5	8	13 038	11
47	12 793	7	12 875	12	13 003	10	13 039	10
79	12 795.5	9	12 879.5	14	13 005	13	13 039	13
138	12 800		12 885		13 005		13 040	
Average thermal shift 7–79 K (10^{-2} cm^{-1} K^{-1})	4.9		12		5.5		5.5	

unusual for zero-phonon R lines of Cr^{3+} impurity centres in ionic crystals, but the R lines of Cr^{3+} in $SrTiO_3$ and $KTaO_3$ show the same behaviour. Moreover, the shift of the A_2 line is unusually large ($\approx$0.11 cm^{-1} K^{-1}), like the shift of the R lines of Cr^{3+} in $SrTiO_3$ at low temperatures (0.19 cm^{-1} K^{-1}), compared to ≈ -0.043 cm^{-1} K^{-1} for Al_2O_3 [29] and ≈ -0.034 cm^{-1} K^{-1} for MgO [30].

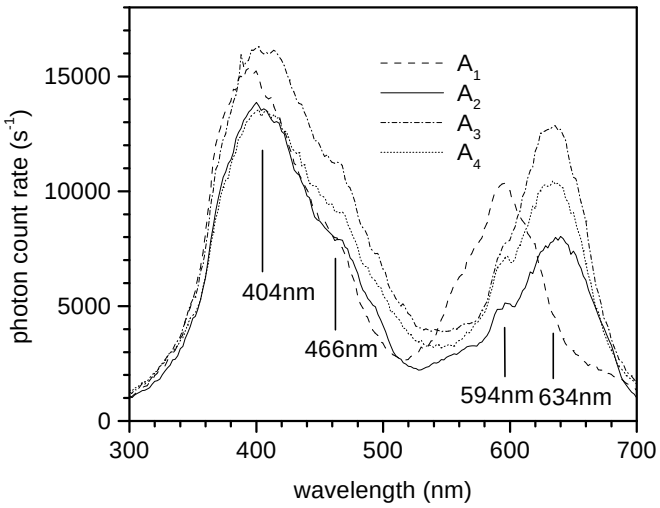

Figure 6. Excitation spectra of the A_1 ($\lambda_{det} = 781.65$ nm), A_2 ($\lambda_{det} = 776.4$ nm), A_3 ($\lambda_{det} = 768.8$ nm), and A_4 ($\lambda_{det} = 766.84$ nm) lines at $T = 74$ K for the $BaTiO_3$:Cr (100 ppm, R32) crystal.

3.3. Luminescence excitation

Figure 6 shows the luminescence excitation spectrum of the A lines for $BaTiO_3$:Cr (100 ppm) at 74 K. It can be seen that the excitation spectra of the emission lines look alike, consisting mainly of two structured bands: Ex_1 with the maximum at 404 nm (3.16 eV), and shoulders at 366 nm (3.38 eV) and at 466 nm (2.66 eV), and another complex Ex_2 excitation band

positioned within the 540–700 nm region, with components centred at 594 nm (2.08 eV) and at 634 nm (1.94 eV). At lower temperature (16.5 K) the same excitation spectrum for the A_{1-3} lines was found. Excitation in these bands results in the structured IR luminescence only.

3.4. Discussion

We suggest that the A_3 and A_4 emission lines may originate from one centre, and can be regarded as the well-known R_1 ($\bar{E} \rightarrow {}^4A_2$) and R_2 ($2\bar{A} \rightarrow {}^4A_2$) lines of 'standard' ${}^2E_g \rightarrow {}^4A_{2g}$ transitions of octahedral Cr^{3+} centres. This conclusion is consistent with the following aspects.

(i) The A_3 and A_4 lines look like a typical doublet. The splitting of the ${}^2E$ orbital doublet of Cr^{3+} at 74 K, caused by the trigonal C_{3v} crystal field, is 34 cm^{-1}, and is therefore of the same order as the values 29 cm^{-1} for Al_2O_3 and 47 cm^{-1} for TiO_2 [11]. The temperature quenching and broadening of the luminescence at $T > 100$ K (see figure 4 and figure 5) are such as to allow no possibility of studying in detail the evolution of this splitting immediately below the phase transition at about 185 K. Because EPR data show nonlocal compensation of octahedral Cr^{3+} in $BaTiO_3$ [12], it looks like a trigonal crystal field represents the main reason for the $A_{3/4}$ line splitting being observed.

(ii) The lifetimes of the A_3 and A_4 luminescence lines are the same, and amount to 0.92 ($\pm$0.06) ms at 70 K, compared with 4.3 ms for Al_2O_3 [31], 11.6 ms for MgO [32], and 18 ms for $SrTiO_3$ (77 K) [1], which is a characteristic millisecond value for the ${}^2E \rightarrow {}^4A_2$ transitions in any host.

(iii) The positioning of the A_3 (768.8 nm, 13 005 cm^{-1}) and A_4 (766.8 nm, 13 039 cm^{-1}) lines at 74 K for $BaTiO_3$ is typical for $R_{1,2}$ lines of Cr^{3+} in perovskite-like and related compounds: 792.9 nm (12 612 cm^{-1}) at 95 K for $SrTiO_3$ [1], and 745.6 nm (13 412 cm^{-1}) at 92 K for $KTaO_3$ [4].

(iv) The IR luminescence spectrum can be understood as well-pronounced zero-phonon lines and multiphonon sidebands, whose intensity ratio is typical for Cr^{3+} emission from the ${}^2E$ state.

(v) Usually the linewidth of the zero-phonon Cr^{3+} lines for ${}^2E \rightarrow {}^4A_2$ transitions hardly changes with the temperature [29, 30]. This is also the case for our $BaTiO_3$:Cr crystals.

(vi) The quenching of the A_4 luminescence line at the lowest temperatures is typical, because this emission comes from the higher excited ${}^2E$ ($2\bar{A}$) state, which is diminished due to the energy transfer from $2\bar{A}$ into the lowest excited $\bar{E}$ state, which is rapid compared to the slow ${}^2E \rightarrow {}^4A_2$ decay with photon emission. At low temperatures, $T < 40$ K, the ratio of the intensities of the $A_{3,4}$ emission lines for insulated Cr^{3+} centres is in good agreement with an approximation of independent insulated electronic luminescence centres with Boltzmann-type distributions for the two ${}^2E$ sublevel populations. At high temperatures, where luminescence thermal quenching effects and related energy-transfer processes have their onset, such an approximation ceases to be satisfactory, which explains the deviation of the ratios of the intensity of the R emission lines from a simple Boltzmann equation prediction.

The rather different properties and nature of the A_1 and A_2 luminescence lines compared with the A_3 and A_4 emission lines have not been quite clear up to now. The relative intensity ratio of the A_1 and A_2 emission lines has been found to be sample independent, supporting the association of the two lines with the same centre. They do show a very similar excitation spectrum with only small deviations in the 540–700 nm region. The

similarity of the excitation spectra hints that there seems to be just the one centre at which all sharp A-line IR emissions originate. Some differences in composition of the components of the Ex_2 band for A_1 and A_2 emission lines could be a consequence of the complexity of the emission excitation mechanisms and of the absorption by other impurity centres in the band gap. It is difficult to relate the positions of the $A_{1/2}$ lines, in view of the weakness of the crystal field, as $^4T_2 \rightarrow {}^4A_2$ zero-phonon lines which appear together with $R_{1,2}$ lines in the luminescence spectrum, like for the Cr^{3+} emission [11] in TiO_2, because:

(i) vibronic sidebands of zero-phonon lines should be more pronounced for such transitions;

(ii) the nature of the Ex_2 excitation band appears unclear; and

(iii) the lifetimes for the $A_{1,2}$ and $A_{3,4}$ emission lines should differ significantly—however, at 70 K the lifetimes of the $A_{3,4}$ lines are similar: 0.92 ($\pm$0.06) ms, while for the A_2 line, 1.34 ($\pm$0.06) ms, and for the A_1 line, 1.21 ($\pm$0.06) ms were measured; i.e. they are different but all remain in the millisecond range.

It is possible that the $A_{1,2}$ emission lines originate from Cr^{3+} centres under exchange interaction with nearest transition metal ions with odd numbers of valence electrons (e.g. Fe^{3+}, d^5). But even more interesting is the possibility of regarding the $A_{1,2}$ lines as originating from pairs of Cr^{3+} centres that are exchange coupled in the nearest B-lattice sites, i.e. as $N_{1,2}$ lines, like those from Cr^{3+} pairs in ruby [33].

Indeed, we can make the following observations.

(i) The shortest distance between neighbouring B sites in the rhombohedral phase of $BaTiO_3$ appears to be $\approx$4 Å, the same value as that for which effective exchange coupling between Cr^{3+} pairs in Al_2O_3 occurs.

(ii) The energy distances between the $R_{1,2}$ lines and the $N_{1,2}$ lines of Cr^{3+} pairs in ruby are nearly the same (for ruby, the energy of the R_1 line is 14 418 cm^{-1}, that of the R_2 line is 14 447 cm^{-1}, that of the N_1 line is 14 204 cm^{-1}, and that of the N_2 line is 14 265 cm^{-1}). Thus, for ruby the $N_{1,2}$ splitting is 61 cm^{-1} (85 cm^{-1} for $A_{1,2}$ lines for $BaTiO_3$:Cr) and the distance to the $R_{1,2}$ lines is of the order of 150–200 cm^{-1}, i.e. practically the same as the distance between the $A_{1,2}$ and $A_{3,4}$ lines for $BaTiO_3$:Cr (160–210 cm^{-1}).

(iii) As was pointed out above, the luminescence lifetimes of $A_{1,2}$ lines are in the millisecond region, typical for $^2E \rightarrow {}^4A_2$ transitions.

(iv) It should be pointed out that not only can Cr^{3+} exchange-coupled pairs appear statistically in $BaTiO_3$:Cr, but also some Cr^{3+} centres can be charge compensated in the crystal growth process by octahedral Cr^{5+} centres in the nearest unit cell, which under photoexcitation of Cr^{5+} can be recharged to Cr^{3+} with the possibility of forming Cr^{3+}–Cr^{3+} exchange-coupled pairs.

Another possible explanation of the nature of the A_1 and A_2 lines is the transition of Cr^{3+} ions situated near to a localized hole, O^- (or other compensators, such as OH^-), where A_1 and A_2 lines originate from A_3, A_4 transitions of Cr^{3+} under the influence of defects in the nearest neighbourhood. The increase of the A_1, A_2 splitting and the shift to lower energies compared with the A_3, A_4 lines could be a result of the action of tetragonal crystal fields of the nearest defects with a favourable relationship between the values and signs of the deformation potentials for the ^2E and $^4A_2$ states of Cr^{3+}.

The nature of the sign of the thermal shift of the Cr^{3+} zero-phonon emission lines of $BaTiO_3$ is not quite clear. For the incipient ferroelectrics $SrTiO_3$ and $KTaO_3$, such a behaviour has been connected in references [2, 3] with a transformation of structure and off-centre behaviour of Cr^{3+} in the photoexcited ^2E state due to a Jahn–Teller effect via

the soft TO-phonon mode. It is not clear to what extent details of this mechanism could be applied to Cr^{3+} in $BaTiO_3$.

The optical absorption and IR luminescence excitation spectra of $BaTiO_3$:Cr are rather too complex for a detailed interpretation to be made. A lot of impurity complexes detected in photo-EPR experiments, mentioned above, can be involved in the excitation and charge-transfer processes. There are no accurate data for the $BaTiO_3$ band gap at low temperatures, due to the masking contributions of fine-domain-structure scattering of the rhombohedral phase (see, e.g., reference [34]). The structure and energy for the optical transitions of Cr^{3+} in $BaTiO_3$ obtained in a theoretical estimation [35] disagree with the results obtained here. The energies of the $^2E \rightarrow {}^4A_2$ and $^4A_2 \rightarrow {}^4T_1$ transitions calculated [35] are 2.11 eV (587.7 nm) and 2.096 eV (591.6 nm) respectively. Hence, the ^2E states should be in the region of the $^4T_2$ band, which is broadened, as is usually argued, by the electron–phonon interaction. Therefore the situation predicted could be comparable to the 'weak-field' situation encountered for $LiNbO_3$, where the main fluorescence band is attributed to the $^4T_2 \rightarrow {}^4A_2$ transition. From energy level diagrams [35], it must also be noted that the occupied $2t_{2g}\downarrow$ level of the doublet excited state of Cr^{3+} should lie rather above the conduction band (CB) edge. This suggests that ^2E or $^4T_2$ states should be unstable or metastable, with a radiative decay competing with the ionization. On the basis of this assumption, in reference [35] the difficulty in observing fluorescence emission for $BaTiO_3$:Cr and the lack of experimental data were both explained. The experimental results presented here yield another picture, and we therefore present a tentative interpretation of the absorption, and the IR emission and luminescence excitation spectra of $BaTiO_3$:Cr.

Using data [36] with reasonable thermo-optic coefficients ($\sim 10^{-4}$ eV K^{-1}), we get 3.13 eV (396.2 nm) for direct- and 2.74 eV (452.5 nm) for indirect-optical-gap transitions at 74 K, which can be connected with the 400 nm excitation band Ex_1 and the absorption shoulder at 470 nm. Therefore, the complex Ex_1 excitation band can be assumed to be related in part to electron and hole creation and Cr^{3+} activation followed by R-line emission caused by charge-transfer processes. Our inspection showed that illumination by light with wavelength $\lambda \geqslant 450$ nm does not increase the photoconductivity; therefore the interpretation of the 466–470 nm absorption band and the IR luminescence excitation corresponding to the $^4A_2 \rightarrow {}^4T_1$ transitions of Cr^{3+} looks plausible.

The absorption and Ex_2 excitation band with a maximum at $\approx$630 nm ($\approx$15 873 cm^{-1}) could be assigned to the $^4A_2 \rightarrow {}^4T_2$ transition of Cr^{3+}. Then the crystal-field parameter Dq can be approximated by the value 1580 cm^{-1}, which is less than the value 1800 cm^{-1} for Al_2O_3 [37], but can be compared with 1550 cm^{-1} for $LiTaO_3$ [6], 1530 cm^{-1} for $LiNbO_3$ [6], and also with $Dq = 1530$ cm^{-1} for $SrTiO_3$, where a 'strong-crystal-field' situation with ^2E as the lowest excited level has been discussed in the literature [1], and which is more related to $BaTiO_3$. As a result, we can estimate the Racah parameter as $B \approx 470$ cm^{-1}, which indicates a moderately high covalency and a strong e–e interaction between weak localized states on the ligands of the d valence electrons of Cr^{3+}. Because of the obvious dependence of the absorption band at around 575 nm in $BaTiO_3$ on the Cr content, following the energy level schemes suggested from photo-EPR results given by Possenriede *et al* [15] and by Schwartz *et al* [21], we assume this absorption to be caused by Cr; that is:

(i) by Cr^{3+} internal transitions ($^4A_2 \rightarrow {}^4T_2$);
(ii) by $Cr^{5+} + h\nu \rightarrow Cr^{4+} + h^+_{VB}$; and
(iii) by $Cr^{4+} + h\nu \rightarrow Cr^{3+} + h^+_{VB}$.

Here $h\nu$ is the photon energy and h^+_{VB} represents a hole in the valence band.

As a result, some part of the Cr^{3+} centres in $BaTiO_3$ situated in Ti^{4+} sites can be

considered to be isolated and nonlocally charge compensated. They result in conventional $R_{1,2}$ zero-phonon emission lines ($A_{3,4}$). But another part of the Cr^{3+} centres at Ti^{4+} sites are initially compensated by Cr^{5+} replacing Ti^{4+} in the nearest unit cells, whose quantity is large enough, according to the EPR data available. Then Cr^{3+} exchange pairs can appear, which can be activated and revealed in emission under excitation by hole ionization and $Cr^{5+} \rightarrow Cr^{3+}$ transformation. It should be pointed out that this picture is in good agreement with photo-EPR data [15], where excitation by light near 600 nm gave rise to hole ionization of Cr^{5+} and Cr^{4+} ($Cr^{5+/4+} + h\nu = h_{VB} + Cr^{4+/3+}$) and rising Cr^{3+} concentration. Thus the nature of the Ex_2 excitation band complexity appears to be clearer, because it includes Cr^{3+} transitions and electron transitions VB $\rightarrow Cr^{5+/4+}$ resulting in the creation of Cr^{3+} exchange-coupled pairs.

Finally we should mention the striking low-temperature lineshape of the inhomogeneously broadened A emission lines, which can be described very well by Lorentz contours, usually typical for narrow homogeneously broadened lines. A discussion of the A lineshape together with results obtained from samples with different chromium contents is under way, and will be presented in a later report [38].

Acknowledgments

The authors are very grateful to A Badalyan for kindly helping with the EPR control measurements. This work was supported in part by NATO HTECH LG 960540, by RFBR Grant 96-02-17972, and by DFG-SFB 225-C7.

References

[1] Stokowski S E and Schawlow A L 1969 *Phys. Rev.* **178** 457
[2] Trepakov V A, Babinsky A V, Vikhnin V S and Syrnikov P P 1988 *Ferroelectrics* **83** 127
[3] Vikhnin V, Trepakov V, Smutny F and Jastrabik L 1996 *Ferroelectrics* **176** 7
[4] Trepakov V A, Babinsky A V, Davydov A V, Syrnikov P P and Jastrabik L 1984 *Sov. Phys.–Solid State* **26** 1885
[5] Burns G, O'Kane D F and Tittle R S 1966 *Phys. Lett.* **23** 56
[6] Glass A M 1969 *J. Chem. Phys.* **50** 1501
[7] Macfarlane P I, Holliday K, Nicholls J F H and Henderson B 1995 *J. Phys.: Condens. Matter* **7** 9643
[8] Fischer C, Kapphan S, Feng Xiqi and Cheng N 1995 *Radiat. Effects Defects Solids* **135** 199
[9] Skvortsov A P, Trepakov V A and Jastrabik L 1997 *J. Lumin.* **72–74** 716
[10] Grabner L and Stokowski S E 1970 private communication, see reference [11]
[11] Grabner L, Stokowski S E and Brower W S 1970 *Phys. Rev.* B **2** 590
[12] Müller K A, Berlinger W and Albers J 1985 *Phys. Rev.* B **32** 5838
[13] Klein M B and Schwartz R N 1986 *J. Opt. Soc. Am.* **3** 293
[14] Possenriede E, Schirmer O F, Donnerberg H J, Godefroy G and Maillard A 1989 *Ferroelectrics* **92** 245
[15] Possenriede E, Schirmer O F, Albers J and Godefroy G 1990 *Ferroelectrics* **107** 313
[16] Possenriede E, Jacobs P and Schirmer O F 1992 *J. Phys.: Condens. Matter* **4** 4719
[17] Possenriede P, Jakobs P, Kröse H and Schirmer O F 1992 *Appl. Phys.* A **55** 73
[18] Schwartz R N and Wechsler B 1993 *Phys. Rev.* B **48** 7057
[19] Schirmer O F, Reyher H-J and Wöhlecke M 1995 *Insulating Material for Optoelectronics* ed F Agullo-Lopez (Singapore: World Scientific)
[20] Scharfschwerdt R, Schirmer O F, Kröse H and Kool Th W 1996 *Ferroelectrics* **185** 9
[21] Schwartz R N, Wechsler B A and McFarlane R A 1992 *Phys. Rev.* B **46** 3263
[22] Hartcock R S, Temple D A and Warde C 1983 *IEEE J. Quantum Electron.* **12** 2122
[23] Müller K A and Berlinger W 1983 *J. Phys. C: Solid State Phys.* **16** 6861
[24] Belruss V, Kalnajs J, Linz A and Folweiler R C 1971 *Mater. Res. Bull.* **6** 899
[25] Müller K A, Blazey K W and Kool T W 1993 *Solid State Commun.* **85** 381
[26] Kool T W, de Jong H J and Glasbeek M 1994 *J. Phys.: Condens. Matter* **6** 1571

[27] Sviridov D G and Boikova A I 1968 *Neorg. Mater.* **4** 468
[28] Aguilar M, Gonzalo C and Godefroy G 1980 *Ferroelectrics* **25** 467
[29] McCumber D E and Sturge M D 1963 *J. Appl. Phys.* **34** 1682
[30] Imbusch G F, Yen W M, Schawlow A L, McCumber D E and Sturge M D 1964 *Phys. Rev.* **133** A1029
[31] Nelson D F and Sturge M D 1965 *Phys. Rev.* **137** A1117
[32] Henderson B and Imbusch G F 1989 *Optical Spectroscopy of Inorganic Solids* (Oxford: Oxford University Press)
[33] Kisluk P, Chang N C, Scott P L and Pryce M H L 1969 *Phys. Rev.* **184** 367
[34] Horie T, Kawabe K and Sawada S 1954 *J. Phys. Soc. Japan* **9** 823
[35] Moretti P and Michel-Calendini F M 1986 *Phys. Rev.* **34** 8538
[36] Cox G A, Roberts G G and Tredgold R H 1966 *Br. J. Appl. Phys.* **17** 743
[37] Wood D L, Ferguson J, Knox K and Dillon J F Jr 1963 *J. Chem. Phys.* **39** 890
[38] Eden S, Kapphan S, Hesse H, Trepakov V, Vikhnin V, Jastrabik L and Gregora I 1998 *Proc. EURODIM (Keele); Radiat. Eff. Defects Solids* at press